

New electroactive macromonomers and multi-responsive PEDOT graft copolymers

Sara Marina^a, Daniele Mantione^b, Kasina Manoj Kumar^c, Kari Vijayakrishna^c, Junkal Gutierrez^{d,e}, Agnieszka Tercjak^d, Ana Sanchez-Sanchez^{*f}, David Mecerreyes^{*a,g}

Received 00th January 20xx,
Accepted 00th January 20xx

DOI: 10.1039/x0xx00000x

www.rsc.org/

Poly(3,4-ethylenedioxythiophene) (PEDOT) is the conducting polymer with the biggest prospects in the field of organic electronics due to its high electrical conductivity and transparency as thin films. It is commonly used and commercialized in the form of aqueous dispersions stabilized by polystyrene sulfonate. However, new PEDOT (co)polymers are necessary with properties such as stimuli-responsiveness, biofunctionality or biocompatibility in emerging application areas such as bioelectronics. Herein, we report for the first time the synthetic pathway towards new propylenedioxythiophene (ProDOT) end-functional polymers or macromonomers and a new generation of multi-responsive PEDOT graft copolymers. First, the macromonomers were synthesized via reversible addition-fragmentation-transfer polymerization (RAFT) mediated by a novel ProDOT based chain transfer agent (CTA). To show its versatility, three different ProDOT end capped macromonomers were synthesized: α -ProDOT-poly(methyl methacrylate) (ProDOT-PMMA), α -ProDOT-poly(ethylene glycol methyl ether methacrylate) (ProDOT-POEGMA) and α -ProDOT-poly(N-isopropylacrylamide) (ProDOT-PNIPAM). Then, the homopolymerization of ProDOT-PMMA macromonomers was carried out by chemical oxidative polymerization obtaining polymacromonomers having semi-conjugated polymer backbone. Finally, the macromonomers were copolymerized with EDOT monomer in water by chemical oxidative polymerization to obtain new graft copolymers. As a result, new PEDOT-graft-POEGMA and PEDOT-graft-PNIPAM were obtained in the form of aqueous dispersions. The graft copolymers were characterized by UV-VIS, FTIR, TEM and AFM showing the typical features associated to electrically conductive PEDOT as well as the phase separation of graft copolymers. Furthermore, the PEDOT-graft-PNIPAM showed thermoresponsive character showing a volume phase transition between 26 and 34 °C depending on the composition and the macromonomer length.

Introduction

In the last decades, electrically conductive polymers have shown great promise in different technologies and as key materials in a number of new devices such as OLEDs, solar cells, organic transistors¹ or electrochromic. Among conducting polymers, poly(3,4-ethylenedioxythiophene) (PEDOT) coupled with polystyrene sulfonate (PSS) is catching more interest day by day due to its high conductivity, easy processing and commercial availability.² Nowadays, PEDOT and related

poly(alkoxythiophene) polymers are also gaining significant attention as materials that can interface between electronics and biology.^{3,4} Their relative low cost, intrinsic conductivity and soft nature compared to traditional metal-based materials makes these conductive polymers (CPs) prime candidates in bioelectronic applications,^{5,6} such as electrodes for electrophysiology,^{7,8} medical diagnosis, organic electrochemical transistors (OECTs)⁹ or neuromorphic computing.¹⁰ Furthermore, functionalization of these conducting polymers can further enhance their advantageous properties such as improved solubility,^{11,12} antifouling behavior, stimuli-responsive switchability¹³, biocompatibility¹⁴ and the ability to modulate cell growth and differentiation.¹⁵ For this reason, there is a growing interest in new PEDOT type monomers or copolymers.¹⁶

Graft copolymers with a conducting polymer backbone and grafts based in a non-conjugated polymer are materials that take advantage of the unique electroactivity, reversible-redox ability, and/or optical properties of the CP backbone completed by chemical and/or physical properties of the grafted sidechains. Graft copolymers can be synthesised by one of three general approaches, namely (i) copolymerization of a macromonomer and a second monomer,¹⁷ (ii) 'grafting from'

^a POLYMAT, University of the Basque Country UPV/EHU, Joxe Mari Korta Centre, Avda. Tolosa 72, 20018, Donostia-San Sebastian, Spain.
Email: david.mecerreyes@ehu.es

^b Laboratoire de Chimie des Polymères Organiques, Université Bordeaux/CNRS/INP, Allée Geoffroy Saint Hilaire, Bâtiment B8, 33615 Pessac Cedex, France

^c Department of Chemistry, School of Advanced Sciences, VIT University, Vellore 632 014, Tamil Nadu, India

^d Group 'Materials + Technologies', Faculty of Engineering Gipuzkoa, University of the Basque Country (UPV/EHU), Plaza Europa 1, 20018 Donostia, Spain.

^e Faculty of Engineering Vitoria-Gasteiz, University of the Basque Country (UPV/EHU), C/Nieves Cano 12, 01006 Vitoria-Gasteiz, Spain

^f University of Cambridge, Dept. of Eng., Electrical Eng. Division, 9 JJ Thomson Avenue, Cambridge, CB3 0FA, UK. * Corresponding authors :

^g Ikerbasque, Basque Foundation for Science, E-48011 Bilbao, Spain

growing the graft from initiation sites in a polymer backbone or (iii) 'grafting to' grafting end-functional polymers into functional groups distributed in a CP polymer backbone.¹⁵ Among these methods, macromonomer method is the simplest way to prepare graft copolymers with regular chain structure.^{18,19} Although there are some examples in the literature about graft copolymers based on conductive polymers like PEDOT/ProDOT,^{20–22} none of them makes use of an alkoxythiophene end-functional macromonomer. Previous examples in the literature have shown the synthesis of electroactive macromonomers bearing pyrrole and mono or tri-thiophenes end-groups *via* conventional and controlled/living polymerizations such as ATRP, ROP or RAFT.^{23, 24, 25} For instance, pyrrole based chain transfer agent (Py-CTA) were developed to obtain pyrrolyl-capped poly-(N-isopropylacrylamide) macromonomers through reversible addition-fragmentation-transfer polymerization (RAFT). In fact, these macromonomers are ideal to copolymerize them with pyrrole, which has a similar reactivity and producing graft copolymers such as PPy-*g*-PNIPAM.²⁶ However, in order to develop the family of PEDOT graft copolymers, the synthesis of alkoxythiophene macromonomers needs to be developed.

The goal of this article is to report the synthesis of a new ProDOT based RAFT chain transfer agent (CTA). This CTA was designed to allow controlling the chemical nature, molecular weight and polydispersity of different ProDOT-macromonomers through reversible addition-fragmentation-transfer polymerization (RAFT). To prove this, three ProDOT end-capped macromonomers, i.e. poly(methyl methacrylate) (ProDOT-PMMA), poly(ethylene glycol methyl ether methacrylate) (ProDOT-POEGMA) and poly(N-isopropylacrylamide) (ProDOT-PNIPAM) macromonomers were synthesized. These grafted polymer sidechains can introduce stimuli-responsive¹³ behaviour or processability¹¹ to PEDOT. Despite the vast variety of thermoresponsive polymers, poly(N-isopropylacrylamide) (PNIPAM) is the most extensively studied as it shows a phase transition from hydrophilic to hydrophobic microstructure, namely *low critical solution temperature* (LCST), when temperature increases above 32 °C, close to the body temperature.²⁷ Similarly, poly(ethylene glycol) (PEG) derivatives have been found to exhibit temperature-responsive behaviour.^{28, 29} In particular, poly(ethylene glycol methyl ether methacrylate)(POEGMA) it is known to be highly biocompatible, water-soluble, nontoxic, and anti-immunogenic.^{30, 31} For these reasons, the homopolymerization and copolymerization of these ProDOT-POEGMA, ProDOT-PNIPAM ProDOT-PMMA, macromonomers with EDOT monomer was investigated *via* oxidative chemical polymerization. As a result, we report in this paper new family of water dispersed temperature responsive PEDOT graft copolymers.

Experimental

Materials

Poly(ethylene glycol) methyl ether methacrylate (OEGMA) (M_n 500) and methyl methacrylate (MMA) were purchased from

Sigma Aldrich and were passed through Micro Polish alumina powder (0.3 μm , BUEHLER) to remove the inhibitors. *N*-isopropylacrylamide (NIPAM, 98%) was obtained from TCI Europe. 3,4-Ethylenedioxythiophene (EDOT, 99%) was acquired from Acros Organics. 4,4-azobis(4-cyanovaleric acid) was recrystallized from methanol and acquired from Sigma Aldrich. All other chemicals, 2,2'-azobis(2-methylpropionitrile) (AIBN, 98%), sodium persulfate ($\text{Na}_2\text{S}_2\text{O}_8$) and iron (III) chloride hexahydrate (FeCl_3), bis-(dodecylsulfanylthiocarbonyl) disulphide, 1,3-dicyclohexyl carbodiimide (DCC) and 4-dimethylaminopyridine (DMAP) were purchased from Sigma Aldrich and used as received. The ProDOT based macro-RAFT chain transfer agent was synthesised, for the CTA part, following the methodology developed by Thang et Al.,³² latterly reported also by Moad et Al.³³ About the transesterification step using ethylene glycol, a procedure from Cortez-Lemus³⁴ was used as guideline. The last step of connection of the ProDOT moiety was reproduced thanks to the procedure previously used in our group, using the available ProDOT-COOH.³⁵ The synthesis and characterization data for the ProDOT based RAFT are included in the Supporting Information. All the solvents used in this work were analytical grade and used without further purification. The Spectra/Por 4 (Spectrumlab) dialysis membrane with MWCO: 12–14 kDa was used to remove salts as well as organic low-molecular weight impurities from dispersions.

Analytical Methods

Nuclear magnetic resonance spectroscopy (NMR). NMR spectra were recorded at room temperature in a Bruker Avance 400 and 500 spectrometers. Chemical shifts are listed in parts per million downfield from TMS and are referenced from the corresponding deuterated solvent peaks.

Size Exclusion Chromatography / Static Light Scattering (SEC/MALLS). SEC/MALS measurements were performed at 30 °C on an Agilent 1200 system equipped with PLgel 5 μm Guard and PLgel 5 μm MIXED-C columns, a differential refractive index (RI) detector (Optilab Rex, Wyatt) and a SLS detector (Minidawn Treos, Wyatt). Data analysis was performed with ASTRA Software from Wyatt. THF was used as eluent at a flow rate of 1 ml/min. dn/dc values in THF were determined using Optilab Rex Detector.

Fourier transform Infrared spectroscopy (FTIR). Infrared spectra were recorded at room temperature with a Thermo scientific model Nicolet 6700 FT-IR spectrometer and KBr pellets were used for solid-state IR spectroscopy applying 10 scans in transmission mode.

Matrix Assisted Laser Desorption Ionization-Time of Flight Mass Spectrometry (MALDI-TOF MS). Mass spectra measurements were performed on a Bruker Autoflex Speed system (Bruker, Germany) instrument, equipped with a 355 nm NdYAG laser. All spectra were acquired in the positive-ion reflectron mode. The polymer samples were dissolved in THF at a concentration of 10 g L⁻¹. Trans-2-[3-(4-tert-Butylphenyl)-2-methyl-2-propenylidene] malonitrile (DCTB, Fluka) matrix was used to acquire the spectra. DCTB matrix was dissolved in THF at a concentration of 20 g L⁻¹ and sodium trifluoroacetate

(NaTFA, Aldrich) was added as cationic ionization agent (approximately 10 g L^{-1} dissolved in THF). Solutions of matrix, salt, and polymer were premixed in the ratio 10:1:10. Approximately $0.5 \mu\text{l}$ of the obtained mixture were hand spotted on the ground steel target plate. For each spectrum, 10,000 laser shots were accumulated. Polytools software (Bruker) was used to calculate the molar mass distribution (MMD) and to identify the end-group structures of the poly-(methyl methacrylate) chains. For the spectra calibration, polyethylene glycol and polystyrene standards were used.

UV-Vis-NIR spectroscopy. UV-Vis-NIR absorption spectra were recorded with a Perkin-Elmer UV/Vis/NIR Lambda 950 spectrometer. For the determination of the *low critical solution temperature* (LCST) of PEDOT-*g*-PNIPAM graft copolymers UV-Vis absorption spectra were recorded with a Shimadzu UV-2550 spectrometer equipped with a CPS-Controller temperature controller.

Differential Scanning Calorimetry (DSC). The DSC measurements were developed using PerkinElmer Pyris 1 calorimeter equipped with a refrigerated cooling system Intracooler 2P, under nitrogen atmosphere flow and calibrated with indium. The sample taken directly from the stable dispersion was weighted and sealed in aluminium pans. The experiment was general conducted in a temperature range between 20 and $70 \text{ }^\circ\text{C}$ at a rate of $20 \text{ }^\circ\text{C}/\text{min}$.

Transmission electron microscopy (TEM). TEM images were collected using a FEI TECNAI G2 20 TWIN TEM, operating at an accelerating voltage of 200 keV in a bright-field image mode. The images were obtain by diluting the dispersions and evaporating into a TEM grid.

Atomic force microscopy (AFM). AFM images were obtained using a scanning probe microscope (Dimension ICON, Bruker) under ambient conditions. Tapping mode was employed in air using an integrated tip/cantilever ($125 \mu\text{m}$ in length with ca. 300 kHz resonant frequency). Scan rates were ranged from 0.7 to 1.2 Hz s^{-1} . Measurements were performed with 512 scan lines and target amplitude around 0.9 V. The amplitude setpoint for all investigated samples was $\sim 300 \text{ mV}$. Different regions of the samples were scanned to ensure that the morphology of the investigated materials is the representative one. In the AFM, phase images the brighter regions correspond to areas of the sample with higher modulus (hard domains) and darker regions correspond to softer areas.

Conductivity. The measurements of conductivity were performed on a four-point probe Veeco/ Miller FPP5000 using layer resistivity function, sampling more than three different zones of the film more than three times and doing the reciprocal. For these purpose, $100 \mu\text{L}$ of each dispersions were drop casted in glass coverslips and dried at room temperature.

Synthetic procedures.

Synthesis of the CTA. In order to obtain the CTA the procedures of Tang et Al.³² and Moad et Al.³³ have been followed. Briefly: dodecanethiol has been condensated with CS_2 , and, then, iodine has been used to create a bis-trithiocarbonate (**1**, Scheme S1). V501 (4,4'-Azobis(4-cyanovaleric acid)) has been use to insert the tertiary cyanoalkyl centre, by releasing

nitrogen, breaking the disulphide bridge and create the carbon-sulphur bond (**2**, Scheme S1). The obtained carboxylic acid derivate has been converted into alcohol by condensing an ethylene glycol moiety *via* Sterling transesterification, as detailed shown in the SI page S3.

Synthesis of ProDOT-CTA. ProDOT-COOH has been obtained by condensing protected bis-MPA and 3,4-disubstituted thiophene ring as previously reported by our team.³⁵ The thus formed ProDOT-COOH and alcohol terminating CTA has been merged using DCC and catalytic DMAP (Scheme S3). The detailed experimental part and the chemical characterizations are reported in the SI.

Synthesis of the macromonomers via RAFT polymerization. A 10 mL Schlenck flask equipped with a magnetic stirring bar was loaded with a mixture of OEGMA₅₀₀ (1 mL, 2.16 mmol), AIBN (7.09 mg, 0.04 mmol) and ProDOT-CTA (27, 8 mg, 0.04 mmol) in 1, 4-dioxane (3 mL) at a molar ratio 50:1:1. The flask was purged of air by applying three freeze-pump-thaw degassing cycles. The magnetically stirred mixture was carried out under inert nitrogen atmosphere at $70 \text{ }^\circ\text{C}$ for 18 h, leading to a yellowish solution. Gravimetric measurements were used to determine the monomer conversion. The macromonomer ProDOT-POEGMA was purified by re-dissolving in dichloromethane and precipitation in cold hexane. Same procedure was developed for molar ratios of 10:1:1 and 150:1:1. The solvent was evaporated to dryness and the ProDOT-POEGMA macromonomer (0.9mg, 84 %) identity was verified using ^1H NMR spectroscopy. ^1H NMR (400 MHz, CDCl_3): δ 0.76-1.06 (br s, CH_3), 1.58-2.07 (br s, CH_2), 3.37 (br s, O- CH_3), 3.64 (br s, O- CH_2), 3.89 (d, 2H, O- CH_2 -C- CH_2 -O, ProDOT-CTA), 4.07 (br s, COO- CH_2), 4.35 (br d, 4H, O- CH_2 - CH_2 -O, ProDOT-CTA), 4.48 (d, 2H, O- CH_2 -C- CH_2 -O, ProDOT-CTA), 6.49 (s, 2 H, S-CH=, ProDOT-CTA). ν_{max} (KBr)/ cm^{-1} 2867 (-CH, st), 1727 (conj. CO, st), 1160 (CO, st), 834 (CS, st). λ_{max} (H_2O)/nm = 310.

To synthesize ProDOT-PNIPAM the same procedure was followed. A 10 mL Schlenck flask equipped with a magnetic stirring bar was loaded with a mixture N-isopropylacrylamide, (750 mg, 6.63 mmol), AIBN (21.8 mg, 0.13 mmol) and ProDOT-CTA (85.4 mg, 0.13 mmol) in 1,4-dioxane (3 mL) at a molar ratio 50:1:1 (Table 1, Entry 5). The resulting yellowish solution after 18h at $70 \text{ }^\circ\text{C}$ was purified by precipitation in cold diethyl ether. Same procedure was developed for molar ratios of 10:1:1 and 150:1:1 but the ratio 10:1:1 was precipitated in cold hexane. The solvent was evaporated to dryness and ProDOT-PNIPAM macromonomer (0.31mg, 79 %) identity was verified using ^1H NMR spectroscopy. ^1H NMR (400 MHz, CDCl_3): δ 0.90 (t, 3H, CH_3 , ProDOT-CTA), 1.17 (br s, CH_3), 1.52-2.06 (br band, CH_2), 3.36 (br s, 2H, CH_2 -S, ProDOT-CTA), 3.91 (d, 2H, O- CH_2 -C- CH_2 -O, ProDOT-CTA), 4.05 (br s, N-CH), 4.37 (br d, 4H, O- CH_2 - CH_2 -O, ProDOT-CTA), 4.51 (d, 2H, O- CH_2 -C- CH_2 -O, ProDOT-CTA), 6.51 (s, 2 H, S-CH=, ProDOT-CTA). ν_{max} (KBr) / cm^{-1} 3309 (NH st), 2971(--H st), 1652 (conj. CO st), 1540 (NH δ), 1370 (-C(CH_3)₂ st). λ_{max} (H_2O)/nm = 310 nm.

For the synthesis of ProDOT-PMMA macromonomers a 10 mL Schlenck flask equipped with a magnetic stirring bar was loaded with a mixture methyl methacrylate (1 mL, 9.35 mmol), AIBN (153.5 mg, 0.93 mmol) and ProDOT-CTA (602.1 mg, 0.93

mmol) in ethyl acetate (3 mL) at a molar ratio 50:1:1. The resulting yellowish solution after 18h at 70°C was purified by precipitation in cold methanol. The reaction was carried out for the synthesis of different molar ratios $[MMA]/[Initiator]/[CTA]$ 10:1:1, 25:1:1 and 100:1:1. The product was dried under vacuum at 50 °C and ProDOT-PMMA macromonomer (0.6 mg, 70 %) identity was verified using 1H -NMR spectroscopy. 1H -NMR (400 MHz, $(CD_3)_2CO$): δ 0.85-1.21 (CH_3), 1.93-2.06 (CH_2), 3.61 (br s, O- CH_3), 3.93 (d, 2H, O- CH_2 -C- CH_2 -O, ProDOT-CTA), 4.40 (br d, 4H, O- CH_2 - CH_2 -O, ProDOT-CTA), 4.48 (d, 2H, O- CH_2 -C- CH_2 -O, ProDOT-CTA), 6.65 (s, 2H, S-CH=, ProDOT-CTA) ppm. $\nu_{max}(KBr)$ / cm^{-1} 1730 (conj. CO, st), 1150-1250 (COC, st), 834 (CS, st). Detailed information about the synthesized macromonomers with different ratios is given in Table 1.

Homopolymerization of ProDOT-PMMA macromonomer. A typical PEDOT synthesis process was carried out for homopolymerization of ProDOT-PMMA macromonomers. A solution of ProDOT-PMMA macromonomer of a mass ratio $[M]/[I]/[CTA]$ (25:1:1) (250 mg) and iron (III) chloride (3 eq. ProDOT-PMMA) in dichloromethane (3 mL) was prepared. The oxidative polymerization reaction was carried out under vigorous stirring at r.t. for 5 days. An obvious phenomenon was observed when the yellowish solution became deep blue coloured during the first hours of reaction. The homopolymer was filtered and then purified by precipitation in cold diethyl ether. The resultant bluish solid was dried under vacuum at 50 °C obtaining gravimetric conversions of 50 %. The detailed information for the homopolymerization of the set of four PMMA macromonomers (Table 1) are given in Table S1.

Synthesis of PEDOT based graft copolymers. The synthesis of graft copolymers was accomplished by the preparation of an aqueous solution of 3,4-ethylenedioxythiophene (50 mg), ProDOT-POEGMA macromonomer of a mass ratio $[M]/[I]/[CTA]$ (50:1:1) (50 mg) and sodium persulfate (1.5 eq. EDOT) in Milli Q water (2.5 mL), followed by the addition of a catalytic amount of iron (III) chloride. The oxidative polymerization was carried out under magnetically stirring at 0°C for 3 days. Instantaneously, upon the addition of iron chloride, the solution turned from yellowish to deep dark blue coloured solution. Finally, the obtained PEDOT-*g*-POEGMA dispersion was dialyzed with deionized water for 48 hours leading a deep dark bluish dispersion.

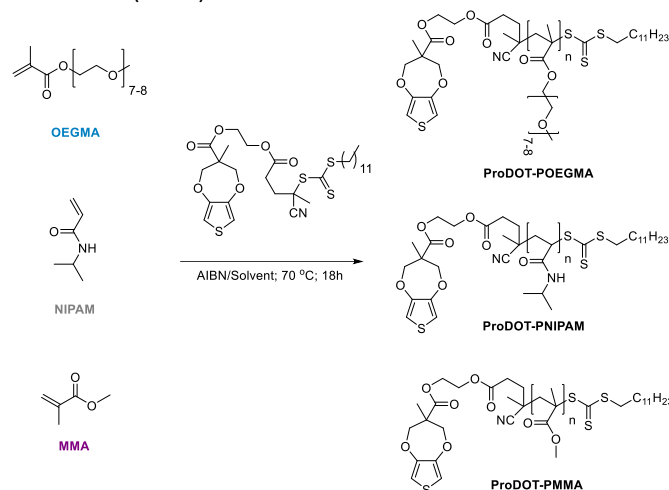
A series of PEDOT based graft copolymer dispersions were prepared with different compositions containing the set of six POEGMA and PNIPAM macromonomers (Table 1) previously synthesized. Detailed information about the compositions are given in supporting information (Table S2).

Results and discussion

Synthesis of ProDOT macromonomers by RAFT polymerization

As mentioned before, the first goal is to develop a new synthetic method for alkoxythiophene electroactive macromonomers. Our proposed synthetic approach relies on the end chain functionality provided by the novel ProDOT RAFT chain transfer agent (ProDOT-CTA). The novel ProDOT-CTA was synthesized by merging two recently reported synthetic pathways. On one

side, following the synthetic procedures developed by Thang et al.³² and Moad et al.,³³ a carboxylic acid-CTA was prepared. By an ethylene glycol moiety, the above-mentioned acid was converted in an alcohol. On the other side, the thiophene based part has been obtained following previous work of some of us, consisting in creating the dioxepine ring by condensating on a 3,4-disubstituted thiophene a protected carboxylic acid-diol.³⁵ The subsequent connection of the ProDOT carboxylic acid moiety to the alcohol-functional CTA was carried out by Steglich condensation to yield the ProDOT-CTA as an orange viscous compound. The synthesis and molecular characterization of the ProDOT-CTA is described in detailed in the supporting information (S1-S6).



Scheme 1. Synthetic procedure for macromonomer synthesis.

Next, the ProDOT-CTA was investigated in the RAFT polymerization of three different acrylic monomers such as OEGMA (ethylene glycol methyl ether methacrylate), NIPAM (N-isopropylacrylamide) and MMA (methyl methacrylate). RAFT polymerization of each monomer was carried out under inert atmosphere in dioxane for NIPAM and OEGMA monomers, and ethyl acetate for the case of MMA, ensuring in both cases the proper solubility of both monomer and RAFT agent. The system was initiated by 2,2'-azobis(2-methylpropanitrile) (AIBN) and mediated by the ProDOT end-capped CTA agent to obtain the functionalization of each macromonomer as illustrated in Scheme 1. We obtained three different macromonomers with different molecular weights by varying the mass ratios between monomer to initiator to CTA ($[M]/[I]/[CTA]$). As shown in Table 1, well-defined macromonomers with relative controlled molecular weights were obtained between 4400 and 24000 ($g\ mol^{-1}$) for ProDOT-POEGMA macromonomers, between 2000 and 20000 ($g\ mol^{-1}$) for ProDOT-PNIPAM and between 1000 and 17000 ($g\ mol^{-1}$) for ProDOT-PMMA. The macromonomers showed in most cases low dispersities between 1.1 and 1.4. The end-group functionalization was confirmed by 1H NMR as the ProDOT end group was readily identified by the presence of the signals at (6.49 ppm) and (4.48 and 3.89 ppm) which were assigned to thiophene and methylene groups, respectively (Fig. 1A). By comparison, the obtained macromonomers molecular weight showed a good correspondence with the expected one

from the monomer to initiator ratio. (Fig. 1A) The macromonomers were also characterized by FTIR confirming its chemical nature (Fig. S10, S12 and S15).

Table 1. Polymerization conditions used for RAFT polymerization of ProDOT-POEGMA, ProDOT-PNIPAM and ProDOT-PMMA macromonomers.

Ent.	DP	[M] ^a	$M_n^{SEC}{}^b$ (g·mol ⁻¹)	$M_n^{NMR}{}^c$ (g·mol ⁻¹)	\bar{D}^d	Yield ^d (%)
1	10	OEGMA	4400	5200	1.3	85
2	50	OEGMA	9700	12700	1.3	84
3	150	OEGMA	24200	-	1.4	80
4	10	NIPAM	-	2000	-	78
5	50	NIPAM	-	10600	-	79
6	150	NIPAM	-	20200	-	63
7	10	MMA	1000	2100	1.7	55
8	25	MMA	6700	-	1.1	70
9	50	MMA	8600	-	1.1	75
10	100	MMA	17600	-	1.1	90

a) Monomer b) Mn determined by SEC in THF using universal calibration according to PS standards, c) Experimental number average molecular weight as measured by ¹H NMR. d) $\bar{D} = M_w/M_n$, e) Calculated as: Yield (%) = (grams of P_i obtained/ grams of monomers in the feed) × 100.

Additionally, MALDI-ToF analysis of the ProDOT-PMMA macromonomers was conducted in order to analyze polymer end-groups (Fig. 1B). As expected, the spectrum provided us the average mass of the MMA repeating unit across the distribution of molecular weight being 100.06 m/z. The spectrum reveals one main population of PMMA chains and some minor populations. Analysis of this main population revealed that the exact mass of the PMMA *n*-mers is in agreement to the presence of chains having a α -ProDOT end-group and a ω -thiocarbonate end group. The excess M_w corresponds to a mass 643.233 m/z, (Fig. S16 and S17) which corresponds to the MW of the initial CTA. The presence of some minor populations is typical of polymers synthesized by RAFT

polymerization and may correspond to AIBN initiated chains, fragmented chains or terminated chains.

Based on above characterizations, ProDOT-POEGMA, ProDOT-NIPAM and ProDOT-MMA macromonomers were successfully synthesized. Next, the homopolymerization and copolymerization with EDOT of these macromonomers will be investigated.

Homopolymerization of ProDOT-PMMA macromonomers

In order to verify the ability to polymerize of these macromonomers, first we investigated the homopolymerization of the ProDOT-PMMA macromonomers. Polymacromonomers are an interesting family of branched polymers as they have one branch per repeating unit. The three ProDOT-PMMA macromonomers with different molecular weights were homopolymerized *via* oxidative chemical polymerization with the presence of a strong oxidant, such as iron (III) trichloride in chloroform (Fig. 2). Over the course of the reaction, a progressive change of color from light yellow to bluish was observed for the whole series of macromonomers. The color of the reaction solutions was stable after 24 h and the reactions were stopped by purification of the products.³⁶

The formation of poly(ProDOT-PMMA) branched polymers was followed by size exclusion chromatography SEC-MALS. In the SEC-MALS traces (Fig. 2), we observed an increase in molecular weights from the macromonomers to the formed polymacromonomers attributed to the self-homopolymerization of the ProDOT end-groups. Decreasing macromonomer molecular weight, lead to polymacromonomers with broader polydispersities and higher molecular weights (Table S1). It is observed that the molecular weight of the polymacromonomer obtained from the polymerization of low molecular weight macromonomer (6700 g mol⁻¹) increased 4.5 times (30200 g mol⁻¹). However, only 1.6 times for the macromonomer of 8600 g mol⁻¹ molecular weight and 1.3 times for the one of 17600 g mol⁻¹. Thus, the polymerization of ProDOT-PMMA macromonomers as in the case of other polymacromonomers it is favoured in the case of

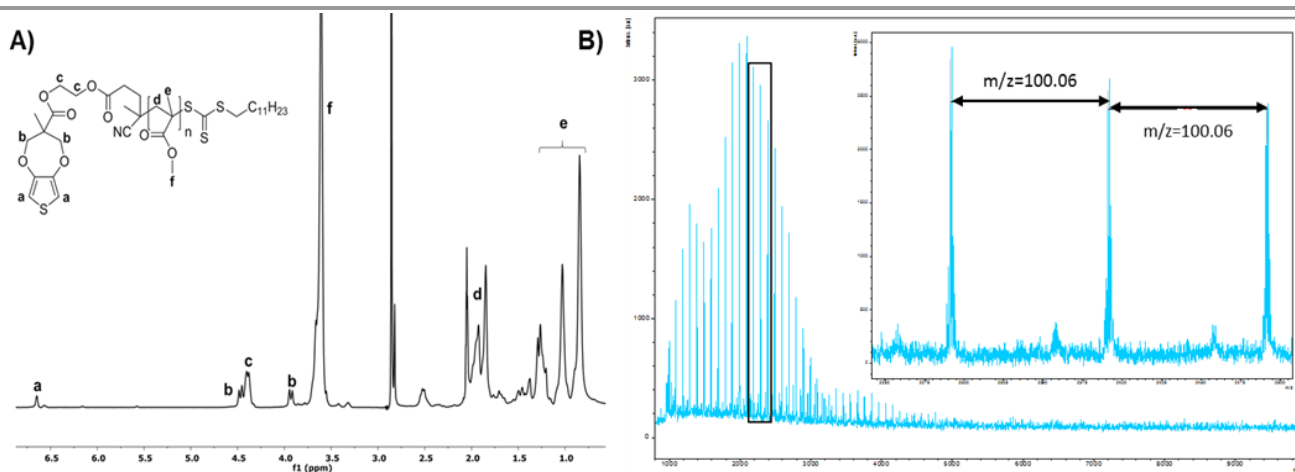


Fig. 1 (A) ¹H NMR spectra of ProDOT-PMMA [M]/[I]/[CTA] ratio (10:1:1) macromonomers. **(B)** MALDI-ToF-MS spectra of ProDOT-PMMA macromonomer of mass ratio of [M]/[I]/[CTA] (10:1:1) with the full spectra and the expanded spectral region.

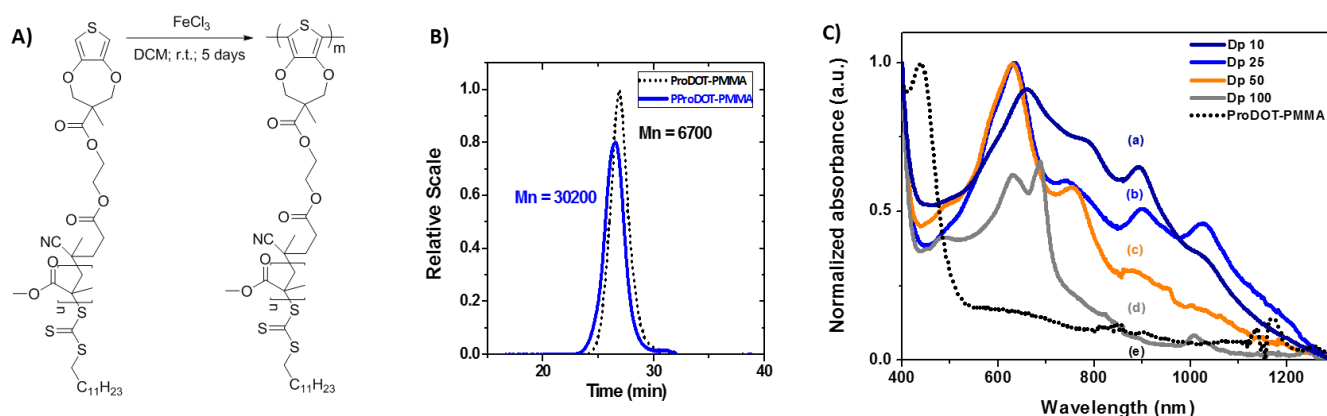


Fig. 2 (A) Scheme of the synthetic chemical oxidative homopolymerization of the PProDOT-PMMA polymacromonomers. (B) SEC-MALS in THF measurements comparison between ProDOT-PMMA macromonomer with a mass ratios [M]/[I]/[CTA] (25:1:1) and the corresponding PProDOT-PMMA poly(macromonomer). (C) UV-Vis-NIR absorption spectra obtained in DCM of (e) ProDOT-PMMA (10:1:1) macromonomer and PProDOT-PMMA polymacromonomers obtained by the homopolymerization of the macromonomers of different [M]/[I]/[CTA] ratios: (a) 10:1:1, (b) 25:1:1; (c) 50:1:1; and (d) 100:1:1.

the low molecular weight ones whereas the high molecular weight macromonomers show difficulties to polymerize.

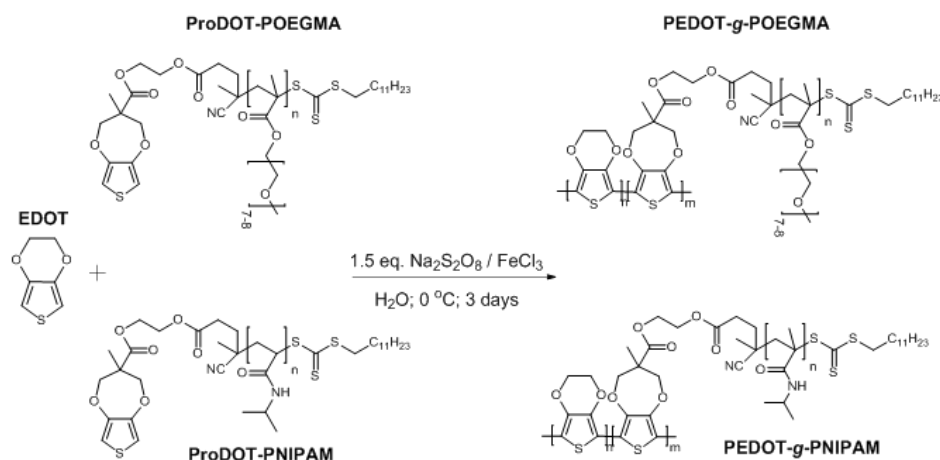
The oxidative coupling between the ProDOT end-groups was verified by UV-Vis-NIR spectroscopy. The initial ProDOT-PMMA macromonomers show an absorption band at 450 nm due to $\pi \rightarrow \pi^*$ transition of the neutral conjugated backbone of the polymer. Upon oxidation, that peak associated to $\pi \rightarrow \pi^*$ transition disappears. Upon polymerization, new peaks and shoulders are observed in the case of the polymacromonomers due to the formation of different oligomers, which was in accordance with the increase in molecular weight (Fig. 2C). For the short polymacromonomer with an average degree of polymerization of 1.3 and 1.8 only two new peaks are observed around 630 and 760 nm. We associated these peaks to the presence of ProDOT dimers and trimers. However, in the case of the long macromonomers with a DP of 4.5 we can observe the peaks at 640, 745, and a broad band with new peaks at 900 and 1025 nm. These peaks could be associated to the formation of the different n -mers such as tetramer and pentamers. This shifting in wavelength of the poly(ProDOT) oligomers is in good agreements with previous reports in the literature^{35,37}

The coupling between ProDOT end-groups was also confirmed by FTIR spectra (Fig. S18). Indeed, the decrease in the intensity of the band at 1350 cm^{-1} , attributed to the double

bond thiophenes was observed, further confirming the polymerization between ProDOT end groups. The band around 872 cm^{-1} and 750 cm^{-1} associated to C-S stretching vibrations bond also undergo an increase in intensity with lower degrees of polymerization.

Synthesis of PEDOT graft copolymers by copolymerization of ProDOT macromonomers and EDOT

Once we verified, that the ProDOT macromonomers were active *via* chemical oxidative polymerization, we investigated its copolymerization with EDOT. In this study, PEDOT-*g*-POEGMA and PEDOT-*g*-PNIPAM copolymers, possessing different compositions and branch lengths, were synthesized macromonomer approach. Therefore, the direct one-step reaction between ProDOT macromonomers and EDOT monomer *via* the oxidation polymerization was developed. The use of sodium persulfate and a catalytic amount of iron (III) chloride in water at $0\text{ }^\circ\text{C}$,³⁸ provided a convenient and general access to PEDOT based polymer brushes of different compositions varying the feeding ratio of ProDOT-POEGMA or ProDOT-PNIPAM macromonomers to EDOT (20:80, 50:50 and 80:20). (Scheme 2 and Table S2). In all the cases, the graft copolymers were obtained in the form of blue aqueous dispersions.



Scheme 2 Chemical oxidative polymerization of the (a) PEDOT-*g*-POEGMA and (b) PEDOT-*g*-PNIPAM graft copolymers.

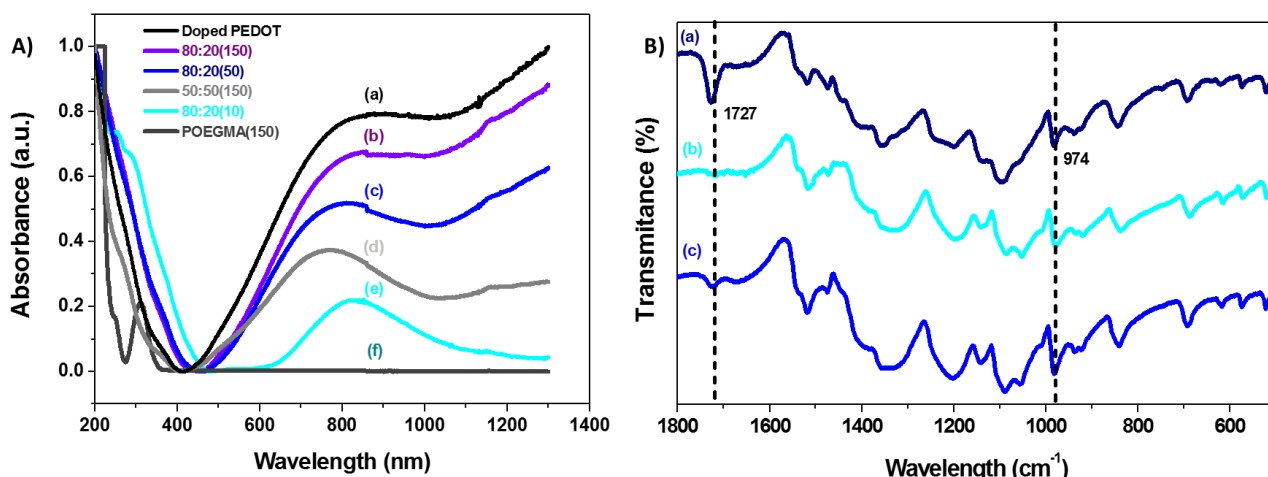


Fig. 3 (A) UV-Vis-NIR absorption spectra of (a) normalized doped PEDOT and PEDOT-*g*-POEGMA copolymers obtained from different weight ratios of EDOT:ProDOT-POEGMA macromonomers of different mass ratios [M]/[I]/[CTA]. (b) EDOT:ProDOT-POEGMA(150:1:1) 80:20; (c) EDOT:ProDOT-POEGMA(50:1:1) 80:20; (d) EDOT:ProDOT-POEGMA(150:1:1) 50:50; (e) EDOT:ProDOT-POEGMA(10:1:1) 80:20 (Table S1); and (f) ProDOT-POEGMA (150:1:1). (B) FTIR spectra of PEDOT-*g*-POEGMA dispersions of ProDOT-POEGMA macromonomer with ratios [M]/[I]/[CTA] (50:1:1). Graft copolymers of followed EDOT: ProDOT-POEGMA (50:1:1) compositions (a) 20:80; (b) 50:50; and (c) 80:20

The chemical structure and electrical properties of PEDOT-*g*-POEGMA and PEDOT-*g*-PNIPAM copolymers were characterized by UV-Vis-NIR and FTIR spectroscopies. It is well known that EDOT monomer presents an absorption maximum at 260 nm leading to well-shaped peak. This band shifts to higher wavelengths ($\lambda_{\max} = 400\text{--}600\text{ nm}$) as EDOT is polymerized and neutral PEDOT is formed.³⁹ The redox state in which PEDOT is presented has huge effect in the absorption spectra. Upon switching PEDOT from its undoped state to the oxidized state, the absorption band at 600 nm due to $\pi \rightarrow \pi^*$ transition decreases as absorption in NIR attributed to the formation of polaron state increases.⁴⁰ Besides some, poorly defined shoulders were detected around 260 nm, all the dispersion revealed that EDOT was polymerized. For the oxidized PEDOT (Fig. 3A(a)) we observed two bands associated to the $\pi \rightarrow \pi^*$ transition at 800 nm and at longer wavelengths a very broad band extended over the NIR region associated to the polaronic state.⁴¹ The same effect was observed for PEDOT-*g*-POEGMA dispersions, which show a polaron in the NIR domains. Deeply analysing the spectra, we observed that as expected higher concentrations of EDOT together with longer macromonomer

side chains lead to more conductive and stable graft copolymers. (Fig. 3A)

FTIR spectroscopy confirmed the presence of both PEDOT and macromonomer units (Fig. 3B). The characteristic bands at 1727 cm^{-1} associated to stretching vibration of the C=O group is observed in the spectra of the graft copolymer. On the other hand, the PEDOT spectrum shows band corresponding aromatic ring vibrations at $1500\text{--}1340\text{ cm}^{-1}$. Bands that appear at $1187\text{--}1083\text{ cm}^{-1}$, are attributed to the C-O-C bending and bands at $974, 834\text{ and }674\text{ cm}^{-1}$ are characteristic of C-S-C stretching vibrations. The FTIR spectrum measured for each family of graft copolymers showed same vibrations bands, and in all of them, we could see transmittance bands related to both PEDOT and macromonomer. Moreover, as shown in Fig. 3B, we could observe some differences when comparing copolymers of different EDOT:ProDOT-POEGMA ratios. As expected, graft copolymers with higher ratios of ProDOT-POEGMA or ProDOT-PNIPAM macromonomers show more intense C=O band (1727 cm^{-1}), whereas the band at 974 cm^{-1} corresponding to PEDOT, became less intense.

Electronic conductivity measurements of the PEDOT-*g*-POEGMA and PEDOT-*g*-PNIPAM thin films obtained by casting

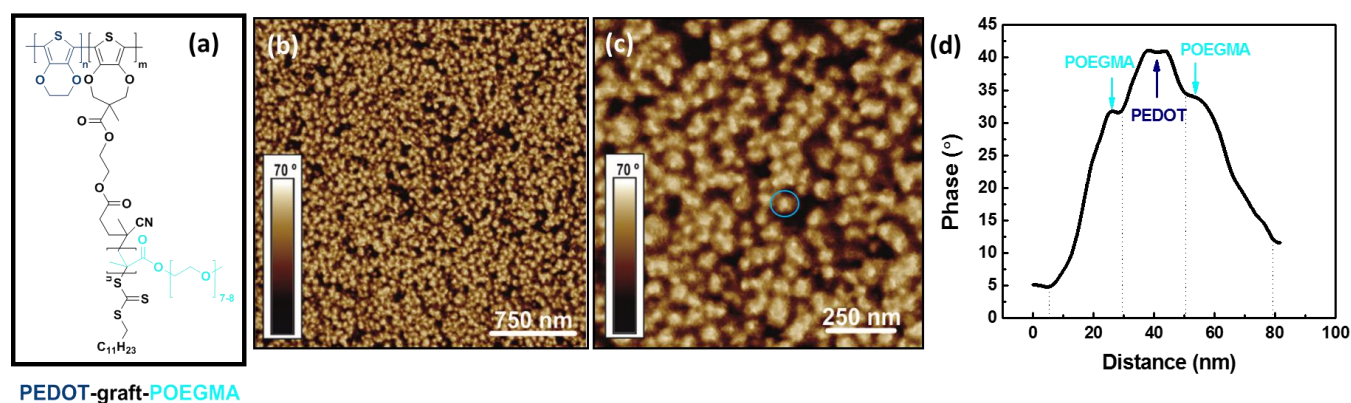


Fig. 4 (a) PEDOT-*g*-POEGMA copolymer molecular structure. AFM phase images of PEDOT-*g*-POEGMA (Table S1, entry 8) with mass ratio 50:50 film based on ProDOT-POEGMA macromonomer [M]/[I]/[CTA] : 150:1:1 mass ratio ($M_n=24200$, Table 1, entry 3) (b) $3\text{ }\mu\text{m} \times 3\text{ }\mu\text{m}$, (c) $1\text{ }\mu\text{m} \times 1\text{ }\mu\text{m}$ and (d) corresponding profile.

the graft copolymer aqueous dispersions were also performed. The obtained electrical conductivity values were in the range of 10^{-2} and 10^{-1} S cm^{-1} , comparable with the electronic conductivity values of pristine PEDOT:PSS whose electronic conductivity has a value of 10^{-1} S cm^{-1} (Table S2).

PEDOT-*g*-POEGMA and PEDOT-*g*-PNIPAM dispersions were further characterized by transmission electron microscopy (TEM). In all the cases, images revealed the formation of quasi-spherical nanoparticles with sizes ranging from 30 to 70 nm. In the case of PEDOT-*g*-POEGMA, the small particles aggregated upon drying whereas in the case of PEDOT-*g*-PNIPAM the nanoparticles appear well distributed into the substrate. (Fig.S20)).

The morphology of PEDOT-*g*-POEGMA copolymer (Fig. 4a) with longest sidechains ($M_n = 24200$ g mol^{-1} , Table S2 entry 8) was analysed by atomic force microscopy (AFM). The dispersions were deposited by drop casting in a glass slides substrate to obtain uniform films of around 10 μm thickness. In order to investigate the homogeneity of the sample, 3 μm x 3 μm AFM phase image was carried out and showed in the Fig. 4b. This AFM phase image indicated a homogeneous structure over the whole investigated surface. Higher magnification AFM images of this copolymer (Fig. 4c) allow distinguishing core-shell morphology, in which bright PEDOT domains form the core surrounded by darker POEGMA side chains shell. This core-shell morphology was also confirmed by AFM phase profile (Fig. 4d). The size of the core was around 20 nm and the shell around 25 nm. It should be mention that the core-shell morphology was uniform in size.

By comparing AFM phase images of different PEDOT-*g*-POEGMA copolymers, one can clearly observed a change in the overall morphology. With increasing macromonomer content from 50:50 to 20:80, higher amount of POEGMA domains are observed appearing as darker zones corresponding to softer domains (Fig S21 (a) and (b)). Morphology change can be attributed to the higher amount of POEGMA soft domains and

the strong interaction between POEGMA side chains. The obtained conductivity is consistent with the insulating nature of POEGMA chains and its predominant presence in the whole surface. (Table S2, entry 4) On the other hand, with increasing PEDOT content, higher amount of PEDOT domains appear in the investigated surface leading to harder domains (Fig S21 (c) and (d)). PEDOT domains become less stabilized by POEGMA side chains creating non-homogeneous distribution over the whole surface. The increase of the PEDOT ratio led to a more granular morphology without covering the entire surface. This heterogeneity has a significant effect on the film conductivity values and the ability to measure them. (Table S2, entry 9).

All in all, the chemical and morphological characterizations confirm the chemical structure of the PEDOT-*g*-POEGMA copolymers. These graft copolymers present typical features of PEDOT (UV-VIS, electrical conductivity) and morphological features of graft copolymers such as the microphase separation and stable dispersions.

As mentioned in the introduction, the graft copolymer strategy can allow introducing different functionality and properties to the PEDOT. For proving this, we investigated the thermoresponsiveness of the PEDOT-*g*-PNIPAM copolymers. This was studied by the method of cloud point⁴² for the determination of the *low critical solution temperature* (LCST). In all PEDOT-*g*-PNIPAM graft copolymers an aggregation of the particles was observed (Table S3) when increasing the temperature above the LCST. In fact, this effect was associated to the physical change undergoing in the polymer as a response to temperature stimuli. An increase in LCST was observed upon copolymerizing the macromonomer with PEDOT. Moreover, higher LCST values are observed when increasing the molecular weight of the macromonomers. Thus, the obtained results range from below room temperature up to 34 °C while increasing sidechains length to higher molecular weights (Table S3). The earlier collapse of copolymers with lower molecular weight branches was also associated to the presence of a higher concentration of ProDOT-CTA, which was insoluble in water. The incorporation of a higher ratio of hydrophobic CTA in the backbone increases the overall hydrophobicity of the macromonomer, resulting in a decrease of the LCST.⁴³ As the PNIPAM content increases, the effect of the RAFT agent becomes less significant.

Additionally, the LCST reversibility for PEDOT-*g*-PNIPAM (20:80) with longer side chains was monitored by differential scanning calorimetry (DSC). The single endothermic heat transition observed was attributed to the dehydration and collapse of the copolymer branches upon temperature change as the water-polymer interactions becomes unfavourable.^{44,45-46} It was observed that the phase transition temperature for PEDOT-*g*-PNIPAM (20:80) is about 33.5 °C, which is higher than the LCST obtained for the corresponding ProDOT-PNIPAM macromonomer at 29.5 °C. (Fig.5) Therefore, graft copolymerization increases the volume transition to higher temperatures.

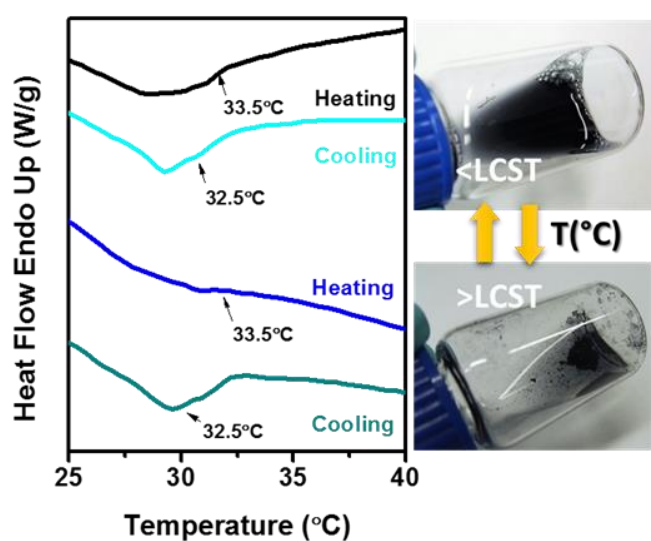


Fig. 5 DSC thermograms of PEDOT-*g*-PNIPAM (20:80) with ProDOT-PNIPAM (table 1, entry 6) macromonomer aqueous solution at two different heating-cooling cycles where both heating and cooling rates were 20 °C/min and the concentration was 1 mg/mL. Polymer agglomerates formed when increasing temperature and re-dissolution upon cooling

Conclusions

A new family of alkoxythiophene end-capped electroactive macromonomers have been synthesized *via* reversible addition-fragmentation (RAFT) using three commercial monomers, MMA, OEGMA and NIPAM. This process could be afforded thanks to the design of ProDOT based CTA agent, which is the first example of a chain transfer agent with ProDOT as end-group. Using ProDOT end-capped electroactive macromonomers fully branched poly(ProDOT-PMMA) copolymers and PEDOT-*graft*-POEGMA or PEDOT-*graft*-PNIPAM water-soluble graft copolymers are obtained. First, the self-homopolymerization of ProDOT-MMA macromonomer was verified by SEC and UV-VIS, showing that the macromonomers with lowest molecular weight have higher ability to polymerize. Next, a series of graft copolymers, PEDOT-*graft*-POEGMA and PEDOT-*graft*-PNIPAM graft copolymers were obtained by chemical oxidative copolymerization between ProDOT terminal functionalized macromonomers and EDOT monomer. The obtained graft copolymers were characterized by a combination of spectroscopic and analysis techniques confirmed the successful oxidation of EDOT for all the cases, showing the best properties for graft copolymer with longest side chains that provided higher stability to PEDOT backbone. Furthermore, the introduction of PNIPAM chains into PEDOT, afforded temperature responsivity to the conductive backbone with LCST values in the range of 26–34 °C. All in all, we demonstrated that the versatility of this method which opens new possibilities to design PEDOT copolymers with (bio)functionality or thermoresponsive behaviour.

Conflicts of interest

There are no conflicts to declare.

Acknowledgements

A. Sanchez-Sanchez is thankful for the Marie Curie IF BIKE Project No. 742865. D. Mantione acknowledge the FP7- PEOPLE-2012-ITN 316832-OLIMPIA. The authors thank for technical and human support provided by SGIker of UPV/EHU and European funding (ERDF and ESF). The authors would also like to thank to José Ignacio Miranda for NMR measurements, Amaia Aguirre Etxebarria for SEC/MALS measurements, Mariano Barrado and Maite Miranda for TEM measurements. S. Marina acknowledge Dr. Jaime Martin for its support and advices.

Notes and references

- 1 S. Inal, J. Rivnay, A. I. Hofmann, I. Uguz, M. Mumtaz, D. Katsigiannopoulos, C. Brochon, E. Cloutet, G. Hadziioannou and G. G. Malliaras, *J. Polym. Sci. Part B Polym. Phys.*, 2016, **54**, 147–151.
- 2 A. V. Volkov, K. Wijeratne, E. Mitraka, U. Ail, D. Zhao, K. Tybrandt, J. W. Andreasen, M. Berggren, X. Crispin and I. V. Zozoulenko, *Adv. Funct. Mater.*, 2017, **27**, 1700329.
- 3 T. Someya, Z. Bao and G. G. Malliaras, *Nature*, 2016, **540**, 379–385.
- 4 J. Rivnay, R. M. Owens and G. G. Malliaras, *Chem. Mater.*, 2014, **26**, 679–685.
- 5 D. Mantione, I. del Agua, A. Sanchez-Sanchez and D. Mecerreyes, *Polymers (Basel)*, 2017, **9**, 354–374.
- 6 D. T. Simon, E. O. Gabrielsson, K. Tybrandt and M. Berggren, *Chem. Rev.*, 2016, **116**, 13009–13041.
- 7 M. Isik, T. Lonjaret, H. Sardon, R. Marcilla, T. Herve, G. G. Malliaras, E. Ismailova and D. Mecerreyes, *J. Mater. Chem. C*, 2015, **3**, 8942–8948.
- 8 E. Bihar, T. Roberts, E. Ismailova, M. Saadaoui, M. Isik, A. Sanchez-Sanchez, D. Mecerreyes, T. Hervé, J. B. De Graaf and G. G. Malliaras, *Adv. Mater. Technol.*, 2017, **2**, 1600251.
- 9 J. Rivnay, S. Inal, A. Salleo, R. M. Owens, M. Berggren and G. G. Malliaras, *Nat. Rev. Mater.*, 2018, **3**, 17086.
- 10 P. Gkoupidenis, D. A. Koutsouras and G. G. Malliaras, *Nat. Commun.*, 2017, **8**, 15448–154462.
- 11 M. Mumtaz, A. de Cuendias, J.-L. Putaux, E. Cloutet and H. Cramail, *Macromol. Rapid Commun.*, 2006, **27**, 1446–1453.
- 12 M. Mumtaz, S. Lecommandoux, E. Cloutet and H. Cramail, *Langmuir*, 2008, **24**, 11911–11920.
- 13 E. Wai, C. Chan, P. Baek, V. R. De La Rosa, D. Barker, R. Hoogenboom and J. Travas-Sejdic, *Polym. Chem.*, 2017, **8**, 4352–4358.
- 14 B. G. Molina, A. D. Bendrea, L. Cianga, E. Armelin, L. J. del Valle, I. Cianga and C. Alemán, *Polym. Chem.*, 2017, **8**, 6112–6122.
- 15 A. J. Hackett, J. Malmström and J. Travas-Sejdic, *Prog. Polym. Sci.*, 2017, **70**, 18–33.
- 16 L. T. Strover, J. Malmström and J. Travas-Sejdic, *Chem. Rec.*, 2016, **16**, 393–418.
- 17 A. Cirpan, S. Alkan, L. Toppare, Y. Hepuzer and Y. Yagci, *J. Polym. Sci. Part A Polym. Chem.*, 2002, **40**, 4131–4140.
- 18 D. Mecerreyes, J. A. Pomposo, A. Bengoetxea M. and G. H., *Macromolecules*, 2000, **33**, 5846–5849.
- 19 D. Mecerreyes, R. Stevens, C. Nguyen, J. A. Pomposo, M. Bengoetxea and H. Grande, *Synth. Met.*, 2002, **126**, 173–178.
- 20 H. Zhao, B. Zhu, S.-C. Luo, H.-A. Lin, A. Nakao, Y. Yamashita and H. Yu, *ACS Appl. Mater. Interfaces*, 2013, **5**, 4536–4543.
- 21 A.-D. Bendrea, G. Fabregat, J. Torras, S. Maione, L. Cianga, L. J. del Valle, I. Cianga and C. Alemán, *J. Mater. Chem. B*, 2013, **1**, 4135–4145.
- 22 J. Malmström, M. K. Nieuwoudt, L. T. Strover, A. Hackett, O. Laita, M. A. Brimble, D. E. Williams and J. Travas-Sejdic, *Macromolecules*, 2013, **46**, 4955–4965.
- 23 Y. Yagci and L. Toppare, *Polym. Int.*, 2003, **52**, 1573–1578.
- 24 A. C. da Silva, T. Augusto, L. H. Andrade and S. I. Córdoba de Torresi, *Mater. Sci. Eng. C*, 2018, **83**, 35–43.
- 25 X.-L. Sun, W.-D. He, J. Li, N. He, S.-C. Han and L.-Y. Li, *J. Polym. Sci. Part A Polym. Chem.*, 2008, **46**, 6950–6960.
- 26 X.-L. Sun, W.-D. He, J. Li, N. He, S.-C. Han and L.-Y. Li, *J. Polym. Sci. Part A Polym. Chem.*, 2008, **46**, 6950–6960.
- 27 L. Zhai, *Chem. Soc. Rev.*, 2013, **42**, 7148–7160.
- 28 Seok Han, A. Mamoru Hagiwara and T. Ishizone*, *Macromolecules*, 2003, **36**, 8312–8319.
- 29 M. M. A. and H. D. H. Ströver, *Macromolecules*, 2004, **37**, 5219–5227.
- 30 Z. Hu, T. Cai and C. Chi, *Soft Matter*, 2010, **6**, 2115–2123.
- 31 J.-F. Lutz, *J. Polym. Sci. Part A Polym. Chem.*, 2008, **46**,

- 3459–3470.
- 32 S. H. Thang, (Bill)Y.K. Chong, R. T. A. Mayadunne, G. Moad and E. Rizzardo, *Tetrahedron Lett.*, 1999, **40**, 2435–2438.
- 33 G. Moad, Y. K. Chong, A. Postma, E. Rizzardo and S. H. Thang, *Polymer (Guildf.)*, 2005, **46**, 8458–8468.
- 34 N. A. Cortez-Lemus, V. Baldenebro, A. Zizumbo-Lopez and A. Licea-Claverie, *Macromol. Symp.*, 2013, **325–326**, 47–55.
- 35 D. Mantione, N. Casado, A. Sanchez-Sanchez, H. Sardon and D. Mecerreyes, *J. Polym. Sci. Part A Polym. Chem.*, 2017, **55**, 2721–2724.
- 36 M. Shiotsuki, W. Zhang and T. Masuda, *Polym. J.*, 2007, **39**, 690–695.
- 37 A. Ali, R. Jamal, W. shao, A. Rahman, Y. Osman and T. Abdiryim, *Prog. Nat. Sci. Mater. Int.*, 2013, **23**, 524–531.
- 38 K. R. Andreas Elschner, Stephan Kirchmeyer, Wilfried Lovenich, Udo Merker, *PEDOT Principles and Applications of an Intrinsically Conductive Polymer*, Taylor & Francis Group, CRC Press., 2011.
- 39 F. N. Ajjan, N. Casado, T. Rebiś, A. Elfwing, N. Solin, D. Mecerreyes and O. Inganäs, *J. Mater. Chem. A*, 2016, **4**, 1838–1847.
- 40 R. H. Karlsson, A. Herland, M. Hamedi, J. A. Wigenius, A. Åslund, X. Liu, M. Fahlman, O. Inganäs and P. Konradsson, *Chem. Mater.*, 2009, **21**, 1815–1821.
- 41 L. Yang, J. Zhang, Y. Shen, B.-W. Park, D. Bi, L. Häggman, E. M. J. Johansson, G. Boschloo, A. Hagfeldt, N. Vlachopoulos, A. Snedden, L. Kloo, A. Jarboui, A. Chams, C. Perruchot and M. Jouini, *J. Phys. Chem. Lett.*, 2013, **4**, 4026–4031.
- 42 H. G. Schild, *Prog. Polym. Sci.*, 1992, **17**, 163–249.
- 43 Y.-C. Chiu, C.-C. Kuo, J.-C. Hsu and W.-C. Chen, *ACS Appl. Mater. Interfaces*, 2010, **2**, 3340–3347.
- 44 R. Bafkary and S. Khoei, *RSC Adv.*, 2016, **6**, 82553–82565.
- 45 L. Klouda and A. G. Mikos, *Eur. J. Pharm. Biopharm.*, 2008, **68**, 34–45.
- 46 J. Niskanen, M. Karesoja, T. Rossi and H. Tenhu, *Polym. Chem.*, 2011, **2**, 2027–2036.